

A Survey of Landscape Metrics and Land-use/land-cover Structures on Urban Heat Islands Surface: A Case Study on Urmia City, Iran

Y. Asadi^a, K. Ezimand^a, H. Keshkar^b, S.K. Alavipanah^{a*}

^a Department of Remote Sensing and GIS, Faculty of Geography, University of Tehran, Tehran, Iran

^b Department of Arid and Mountainous Regions Reclamation, Faculty of Natural Resources, University of Tehran, Karaj, Iran

Received: 30 March 2019; Received in revised form: 17 October 2019; Accepted: 26 October 2019

Abstract

Urbanization is developing unprecedentedly on a global scale. One of the chief repercussions of urbanization, caused by man-made alterations in land-use/land-cover (LULC), is the formation of urban heat islands. Albeit, differences among landscape structures and its accompanied effects on the environment are mostly neglected. Accordingly, the main objective of this study is to survey the various effects of LULC on urban heat island in terms of landscape metrics. For this purpose, Landsat-8 images and land-use maps extracted for the study region (Urmia) were employed. Landscape metrics were calculated from Landsat images with spatial resolution of 30 m for five varying scenarios (residential lands of five-floors and more, residential lands with less than five-floors, administrative-commercial lands, industrial lands, educational and health lands). The metrics were then investigated with respect to two types of land-cover (vegetation and impervious lands). Analysis results indicate that following industrial use, administrative-commercial use is the most significant factor contributing to the formation of heat islands. Results also stipulated the indirect relationship between vegetation and land surface temperature for all scenarios, with the exception of industrial use; in contrast impervious surfaces showed a direct relationship with earth temperature. Study results further determined the effectiveness of human factors in conjunction with LULC as amongst key factors influencing urban LST. Finally, the study specified how different effects of LULC on heat island of Urmia can be well defined with reference to landscape metrics.

Keywords: Landsat Images; Landscape Metrics; Land-use/Land-cover; Urban Heat Islands; Urmia city

1. Introduction

Urban heat island is a phenomenon by which urban environments tend to show higher temperatures than their surrounding rural environments (Liu and Zhang, 2011; Yousefi *et al.*, 2015). The phenomenon is itself known to be caused by other urban environmental events as well as increases in human population (Li *et al.*, 2011; Nonomura *et al.*, 2009), expansion of built up lands (Ezimand *et al.*, 2018) and LULC transformations in urban areas (Li *et al.*, 2016; Alavipanah *et al.*, 2017). Generally, there are two approaches to the study of urban heat islands (Streutker, 2003). The first method proceeds

towards measuring temperature data at meteorological stations. Although differences in temperature between urban and suburban areas can be measured using weather station data, it is not possible to generalize the measured heat difference as a single point for all areas. On this ground, use of satellite images have been considered for the study of heat islands and LST (de Faria Peres *et al.*, 2018) as they simultaneously provide a comprehensive coverage of the entire city as well as the suburbs (Streutker, 2003).

Remote sensing images have also been considered as satisfactory sources of information for the preparation of thermal maps and other applications regarding the accurate examination of climate change, urban heat island and land-use in urban and suburban areas, due to their various features including extensive and continuous

* Corresponding author. Tel.: +98 21 8896 5582
Fax: +98 21 8896 4917
E-mail address: Salavipa@ut.ac.ir

coverage, regular time series, timeliness, and the ability to obtain information in the reflectance and thermal fields of electromagnetic waves (Hakimzadeh Ardakani and Vahdati, 2018; Weng *et al.*, 2004; Weng, 2009).

Vegetation and impervious surfaces are two major areas of interest in urban structure (Rimal *et al.*, 2018). Estimation of impervious land surfaces (walkways, roads, parking lots) is monumental and extremely functional for determining heat differences in urban environments (Arnold and Gibbons, 1996). Vegetation, through evaporation and transpiration-perspiration reduces the effects of urban heat island (Weng, 2001; Goward *et al.*, 2002) and therefore has significant effects on land surface temperature (LST) (Yuan and Bauer, 2007; Quan *et al.*, 2014).

Time-space changes of LULC also influence temperature processes (Shen *et al.*, 2016). Urban landscapes encounter diverse surface features due to complex heterogeneity of LULC (Kourosh Niya *et al.*, 2019; Rimal *et al.*, 2019a). This heterogeneity in spatial patterns and physical, environmental, social, and economical processes inside urban borders can affect heat patterns within a city (Luck and Wu, 2002). Therefore, it is necessary to consider the relation of urban spatial patterns in conjunction with environmental processes to help better understand urban ecosystems.

Different methods have been investigated for the study of spatial and temporal variations of thermal patterns (Cenedese and Monti, 2003). Some studies have employed island heat intensity to understand temporal changes (Han-qiu and Ben-qing, 2004), while others have employed regression and hotspots to examine heat islands (Bruns and Simko, 2017). Statistical analysis methods have also been used to identify spatial variations of heat islands (Xunqiang *et al.*, 2011). Advanced numerical and physical models are amongst other methods developed to study surface temperature of cities (Streutker, 2002).

Numerous studies have focused on the effects of LULC on patterns of temperature change. Xiao and Moody (2005) studied the relation between LULC and LST patterns in Southern China using TM and ETM+ images. The results indicated that higher temperatures in urban areas had a direct relationship with LULC. Weng *et al.* (2007) proposed a successful method for

determining the relationship between LST, land-use patterns and land-cover using remote sensing data and ecologic landscape methods. Nonomura *et al.* (2009) surveyed heat island effects of Takamatsu with regard to vegetation and increased human population. They concluded that heat island formation elevates in areas with decreased vegetation and expanding human population. In Iran, Amiri *et al.* (2009) studied the spatial and the temporal variations of surface temperature in relation to land-use and changes in vegetation in Tabriz. The results indicate the effective role of vegetation in modulating land surface heat and how land-use changes caused by urbanization lead to the increase of urban temperatures. The focal point for most previous studies on heat islands was LULC, however, considering the significant effects of economic and social activities of human beings on the urban environment, vegetation and land-use patterns alone cannot provide sufficient grounds for the accurate examination of heat islands.

Urmia has been developing horizontally and irrationally in recent years, which in turn has led to the loss of green space and the transformation of natural lands into built up lands, followed by the expansion of urbanization and increased LST. Therefore, this study seeks to identify and investigate the varying effects of different types of LULC on urban heat islands, specifically, the effects of human activities on the heat island of Urmia.

2. Materials and Methods

2.1. Study area

Urmia, the capital of West Azerbaijan province, is located alongside the Urmia Lake. This city is located in 37° 4' latitude and 45°, 4' longitude (Fig. 1). According to the 2011 census, with a population of 667,499, Urmia is the tenth most populated city in Iran. With an elevation of 1332 m, it is located on the western side of Urmia Lake. The climate of the city, mainly influenced by latitude, vicinity to Urmia Lake, elevation and moist Mediterranean air currents, is hot during the summers and cold during winters (Javan and Malazadeh, 2013). In recent years, irregular growth of urban population as a result of immigration has led to vertical developments within the city based on no particular pattern.

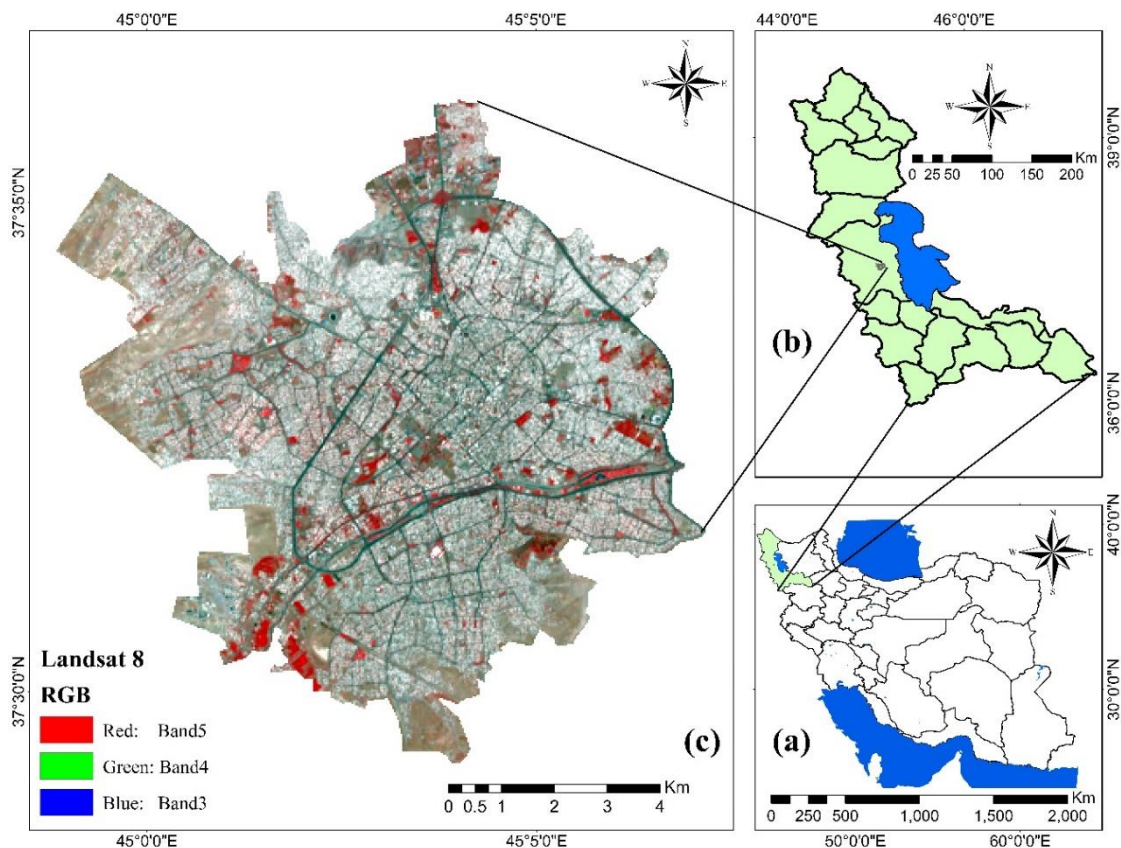


Fig. 1. Introduction of the study area (a) location of west Azerbaijan province (b) location of Urmia city regarding the province (c) false color composition of Urmia city

2.2. Data collection and pre-processing

Landsat-8 images were used as the main source of data for this study. The images are located in route 169 and in row 34 of Worldwide Reference System (WRS). OLI/TIRS sensory images from July 18, 2015 including 11 radiometric bands were also selected. Image selection was carried out by considering certain inclusion criteria including time constraints (summer), desirable quality and lack of cloud cover on image. Different effects of LULC on land surface temperature changes were examined for summer using images from July 18th, 2015, mainly due to the fact that the heat island of Urmia peaks in intensity during this season.

This image was atmospherically corrected in course of pre-processing (Keshtkar *et al.*, 2017). All pre-processing steps were processed in an ENVI 5.3 environment (Exelis Visual Information Solutions, Boulder, Colorado). In this study, L1T image was converted from digital number (DN) to radiance and image processing functions were conducted applying the radiometric calibration model. The FLAASH atmospheric correction model was employed using radiance image by applying the appropriate

model on the location of the study area (Rimal *et al.*, 2019b). Geometric adjustments were initially performed in accordance with topographic maps of Urmia city at a 1:25000 scale and the positional root mean square (RMS) error of geometric rectification was not more than 0.5 pixels.

In order to analyze different effects of land-uses on heat islands, information layers of five built-up features – i.e. five-floors and more (FFM), less than five-floors (LFF), workshops-industrial, administrative-commercial, educational and health-care departments- were used. The corresponding data were procured from the municipality of Urmia (Fig. 2). Ultimately, 528 health education units, 199 industrial workshop units, 7287 administrative commercial units, 9619 residential buildings of LFF, and 90 units of FFM were considered for further investigations.

2.3. Estimation of LST

Spectral radiance is defined as the amount of reflected energy observed by a sensor above the atmosphere. Spectral radiance for all Landsat-8

bands was calculated using equation 1 (USGS, 2013).

$$L_{\lambda} = M_L * Q_{cal} + A_L \quad (1)$$

, where M_L and A_L are the band-specific multiplicative and additive rescaling factors from the metadata, respectively; and Q_{cal} is the quantized and calibrated standard product pixel values (DN).

Obtaining LST requires the calculation of brightness temperature related to Landsat thermal bands, which can be obtained according to the following (equation 2) (USGS, 2013):

$$TB = \frac{K_2}{\ln\left(\frac{K_1}{L_{\lambda}} + 1\right)} \quad (2)$$

, where TB is the at-satellite brightness temperature (K); L_{λ} is the spectral radiance at the sensor's aperture in w/(meter squared sr μm); and K_1 and K_2 are the band-specific thermal conversion constants from the metadata. LST was then calculated as so (equation 3) (Artis and Carnahan, 1982):

$$LST = \frac{TB}{1 + (\lambda \times TB / \alpha) \ln(\varepsilon)} \quad (3)$$

, in which TB is the satellite brightness temperature in K; λ is the wavelength of the emitted radiance in meters; $\alpha = 1.438 \times 10^{-2}$ mK; and ε is the surface emissivity.

Emissivity for water (NDVI less than zero), soil (NDVI between zero and 0.15) and plants (NDVI over 0.15) were 0.9925, 0.923, 0.727, respectively (Xie et al., 2012). Other values of NDVI were modelled using equation 4 (Van de Griend and Owe, 1993).

$$\varepsilon = 1.0094 + 0.047 \ln(NDVI) \quad (4)$$

2.4. Land-cover map preparation

Urban landscapes in this study have been categorized into different LULC, using Images from OLI/TIRS sensors related to 18th July 2015. Impervious surfaces (asphalt, concrete, brick and so on) and vegetation were the two main categories of land-cover (Fig. 2). Signals registered by the sensor in urban environments were related to different reflections of several

sensors. There are several methods for elicitation of built up lands or impervious land-cover based on remote sensing images (Ezimand et al., 2018), each of which lead to different results depending on the type of area and signature of each spectrum (Estoque and Murayama, 2015). Moreover, these methods use a specific band for classification. Accordingly, this study used the Normalized Spectral Mixed Analysis (NSMA) method proposed by Wu (2004) to extract impervious lands. The method works by calculating the average of all bands and then dividing each band by their corresponding average value in order to reduce the brightness difference in the spectra of a given material. Pixel values are normalized according to equations 5 and 6.

$$\bar{R}_b = \frac{R_b}{\mu} \times 100 \quad (5)$$

$$\mu = \frac{1}{N} \sum_{b=1}^N R_b \quad (6)$$

, where \bar{R}_b is the normalized reflectance for band b in a pixel; R_b is the original reflectance for band b; μ is the average reflectance for the corresponding pixel; and N is the total number of bands. After normalization, NSMA can be calculated using equations 7 and 8 as so:

$$\bar{R}_b = \sum_{i=1}^N \bar{f}_i \bar{R}_{i,b} + e_b \quad (7)$$

$$\sum_{i=1}^N \bar{f}_i = 1 \text{ and } \bar{f}_i \geq 0 \quad (8)$$

, where \bar{R}_b is the normalized reflectance for each pixel in band i ; $\bar{R}_{i,b}$ is the normalized reflectance of endmember i in band b for that pixel; \bar{f}_i is the fraction of endmember i and e_b is the residual (Wu, 2004).

NDVI index was used to extract vegetation regions. The NDVI index is perhaps the most popular, straightforward and practical indicator used in numerous studies to analyze changes in land-cover, including vegetation (Keshtkar et al., 2013). To estimate this index, infrared bands (band 4) and infrared bands near to band 5 of

Landsat-8 images were used. NDVI was calculated using equation 9 as follows (Rouse Jr et al., 1974).

$$NDVI = \frac{\rho_{NIR} - \rho_{Red}}{\rho_{NIR} + \rho_{Red}} \quad (9)$$

, where ρ_{NIR} is reflectance values of near infrared band and ρ_{Red} is reflectance values of the red band. The vegetation index ranges from -1 and +1, with negative values indicating areas with no vegetation and values over 0.15 used for areas with vegetation (Keshtkar, 2008).

The accuracy assessment process, as with previous studies, has been performed using reference points in a random manner. These points vary in numbers from several hundred (Estoque and Murayama, 2013) to several thousand (Du et al., 2014). For this study, 500 points were obtained using panchromatic images which provide higher spatial resolution compared to multispectral bands and can be used to evaluate accuracy (Du et al., 2014). A random sampling method was used to select the data. The classification accuracy of the land-cover map was evaluated using *confusion matrix*. The overall accuracy of the classification for land-cover was obtained as 88.8%.

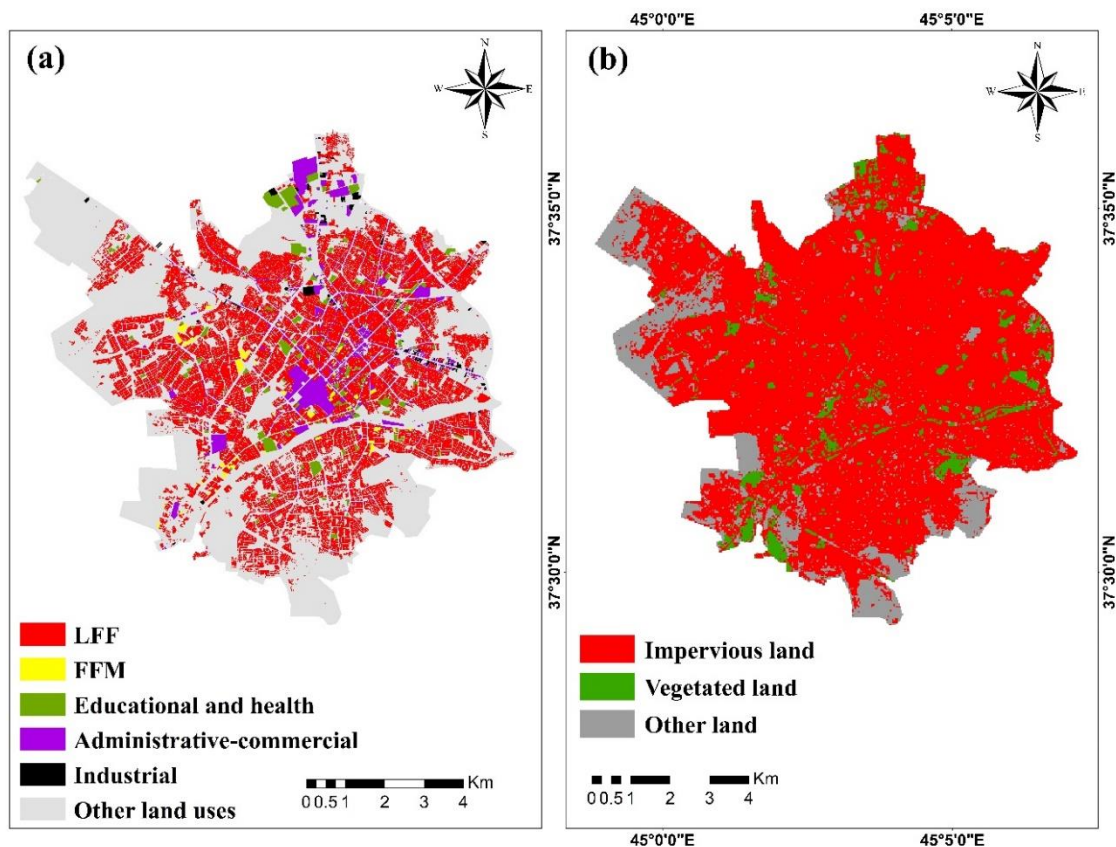


Fig. 2. (a) data layers of different land-uses (b) land-cover map prepared by NSMA method

2.5. Calculation of landscape metrics

Since landscape ecology emphasizes on interaction between spatial patterns and ecological processes, proving methods in which spatial patterning can be defined and quantitatively determined is necessary (Turner et al., 2001). Quantitative surveys of composition and spatial distribution of landscape structural elements is possible through the use of landscape metrics. Landscape metrics are algorithms for quantifying special spatial characteristics of

patches, classes or overall landscapes (McGarigal et al., 2002). Selecting the proper metrics is highly dependent on landscape properties and ecological characteristics of an area (Kong and Nakagoshi, 2006). Selection of the metrics in this research is based on their importance, landscape properties and also recent similar studies (e.g., Li et al., 2011; Li et al., 2014; Li et al., 2013). This study used five landscape metrics as shown below (Table 1).

The PD metric is used to study the density of pieces (patches) and is equal to the total number

of patches related to one kind of patch divided by total area of landscape multiplied by 10000 to convert to hectares and is always bigger than zero (Li *et al.*, 2014). This facilitates the comparison of different uses with different surfaces. As the distance between density and used pieces decrease, LST rises and the effects of unfavorable atmospheric conditions (including fire,...) on land-uses increases resulting in inappropriate environmental conditions (Turner *et al.*, 2001). The ED metric is defined as the perimeter of each piece of land relative to the area of the landscape, which is used to measure

the complexity of the shape of a piece in the landscape. Increasing values of this metric will cause further tears in natural land-cover and dispersion of applications in the region as well as different heat patterns (Turner *et al.*, 2001). PLAND metric represents landscape percentage. It is obtained as the total area (m²) of all pieces related to a single type of piece divided by the total area of the landscape (m²) multiplied by 100 to convert to percentage (Li *et al.*, 2011). The LPI metric (the area of biggest latches) shows the spatial area of land-cover in landscape surface (Turner *et al.*, 2001).

Table 1. Five landscape metrics used in this study

Variable	Unit	Range	Description	Formulas
Percentage of Landscape area (PLAND)	%	0<PLAND<100	Percentage of the area of a particular patch type of total landscape area	$\frac{100}{A} \times \sum_{i=1}^n a_i$
Patch density (PD)	Number per ha	PD > 0	Number of all patches at the given class divided by total landscape area	$\frac{n}{a} \times 10^4$
Mean patch size (MPS)	ha	MPS > 0	Average patch size	$\frac{\sum_{i=1}^n a_{ij}}{n_i} \left(\frac{1}{10000} \right)$
Largest patch index (LPI)	%	0<LPI<100	Percent of the total landscape that is made up by the largest patch	$\frac{\max_{a_j}}{A} \left(\frac{j=1, n}{100} \right)$
Edge density (ED)	m/ha	ED > 0	Amount of edge relative to the landscape area	$\frac{10000}{A} \times \sum_{k=1}^n e_{ik}$

The MPS metric is defined as the average area of the pieces for each particular user. Higher values for the range of the area of the pieces around the average, indicate that the pieces are composed of more varied surfaces, and the disposition and human involvement in these uses has been high over time (Li *et al.*, 2014). Landscape metrics, depending on the type of land-cover, have a different relationship with the thermal pattern (Maimaitiyiming *et al.*, 2014; Li *et al.*, 2013).

3. Results

3.1. Variety of LST for different LULC

The LST map for different LULC of Urmia city is presented in figure 3. As can be seen from the figure, temperatures changes varied from 20.60 to 39.3°C in 18th July, 2015 (Fig. 3). The

average temperatures for different land-uses are shown in table 2. It can be observed that among five different land-uses, industrial area has the highest thermal average (30.50°C), followed by administrative-commercial type (30.45°C), educational-health (30.40°C), FFM residential (29.4°C) and LFF residential with the least thermal average (27.65°C) (Table 2).

Most lands in the study region were of LFF residential type, which has the lowest average temperature, whereas lands with FFM residential cover showed the least contribution, ranked fourth in terms of average temperature. Industrial land-uses contribute to the smallest area following FMM residential lands and have the highest temperature. In this regard, large contributions of administrative-commercial covers with high temperatures can play an important role in the heat island of Urmia.

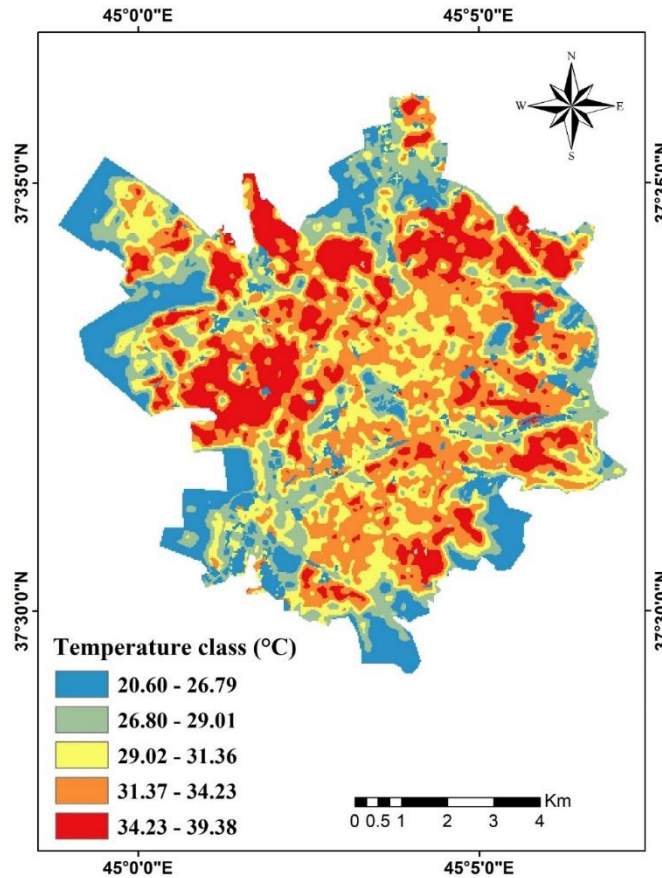


Fig. 3. Temperature of LULC of Urmia city related to 18th July, 2015

Table 2. The standard deviation and temperature of five different land-uses

Land-use types	Area (ha)	Mean (°C)	Standard deviation
Industrial	50.01	30.50	3.54
Administrative-commercial	413.29	30.45	2.62
Educational-health care	207.12	30.40	2.52
FFM residential	42.79	29.04	1.35
LFF residential	2462.56	27.65	1.89

3.2. Relationship between LST and different LULC types

As shown in figure 2, impervious surfaces (%79.75) expand much further compared to vegetation (%6.02), which could intensify the impact of impervious surfaces on LST compared to vegetation cover. In addition, the layout of the land-cover is significantly effective on LST. Therefore, the main determinant of surface temperature in the city of Urmia is impervious lands, which are large in area and form interconnected parts.

LST in industrial areas, with 3% vegetation and 94% impervious surfaces is quite different from educational-health care lands with the same amount of vegetation and impervious surfaces. The temperature inconsistency between these two factors is the result of the heat obtained from

burning fossil fuels as well as the pollution produced by industries, which increase the affectivity of impervious surfaces in industrial areas compared to educational-health lands.

The percentage of green space in commercial use (18%) is significantly more than industrial use (3%) and the percentage of impervious surfaces in administrative-commercial use (81%) is less than the percentage of impervious surfaces in industrial use (94%); however, considering the difference in vegetation percentages among these two land-uses as well as the percentage of impervious lands, there seems to be no significant difference in LST level among these land-covers, which itself looks to be the results of increased human activities in administrative-commercial areas compared to industrial lands. This indicates the importance of human activities in creating urban heat islands.

Comparison of the temperature of LFF residential and FFM residential lands shows that vegetation percentage in LFF residential (2%) is considerably (five times) less than vegetation in FFM residential (10%). In addition, the percentage of impervious surfaces in LFF residential (98%) is considerably and clearly more than the percentage of FFM residential lands (89%). Based on these results, LST in LFF residential lands should be higher than LST of FFM residential lands, which contradicts the results of table 2. This difference is obviously due to vertical growth of buildings (FFM residential areas), followed by the impact and significance of various human activities (body metabolism, ventilation, and more heating equipment, etc.) on LST in residential areas with high-rise buildings of more than 5 stories. These results are also indicative of the contraction of land-cover in different land-uses (FFM residential to LFF residential areas).

As shown in table 2, administrative-commercial land-uses has a higher thermal average compared to educational-health land-use. Due to high temperatures in administrative-commercial lands, in addition to wide impervious lands, which have a high thermal capacity, populations are also high, as a result of which heat emission from human activity in

administrative-commercial lands is higher than educational-health care lands. Also, the percentage of vegetation in educational-health lands is greater than administrative-commercial areas. Due to the effect of vegetation on reducing temperatures, educational-health care lands show a lower thermal average compared to administrative-commercial lands.

It should also be taken into account that educational-health lands contribute more in total area and green spaces (Table 2) compared to administrative-commercial lands with less population density, which has lowered the average temperature in educational-health lands. Vertical growth of structures, types of materials, anthropogenic heat production, increasing number of floors in residential and expanding human resources all contribute to the increase of LST. This thermal difference is completely obvious in LFF and FFM residential areas. This considerable impact has resulted in a higher priority for FFM residential areas compared to LFF lands. These results indicate the impact of human activity as well as increases in the number of floors of buildings on surface temperature. Table 3 shows Pearson correlation analysis between LULC to identify contradicting effects of LULC on LST.

Table 3. Partial correlation between LST and land cover composition and configuration metrics of the five land-use types

	Educational-Health	Ministerial-Commercial	Industrial	FFM	LFF
<i>Vegetated land-cover</i>					
PLAND	-0.290	-0.073	0.103	-0.176	-0.024
PD	-0.285	-0.135	0.152	-0.269	-0.090
MPS	-0.447	-0.058	0.613	-0.191	-0.276
ED	-0.294	-0.089	0.096	-0.190	-0.022
LPI	-0.285	-0.035	0.152	-0.269	-0.099
<i>Impervious land-cover</i>					
PLAND	0.177	0.473	0.044	0.140	0.015
PD	0.099	-0.324	0.041	0.093	0.019
MPS	0.316	0.214	0.155	0.056	0.011
ED	0.065	0.272	-0.047	0.148	0.015
LPI	-0.099	0.324	0.041	0.093	0.019

As noted above, PLAND examines the percentage of different coatings. The relationship between green vegetation and all land-use with LST, with the exception of industrial use, has been negative. With increasing green vegetation cover, PLAND value has increased and the highest correlation between vegetated land-cover and surface temperature in Educational-Health has been due to increasing vegetation percentage at this site. The cause of the positive correlation

between vegetation and the LST in industrial use is due to the decrease in the percentage of vegetated land-cover relative to the impervious surface. The relationship between urban impervious surfaces in different land-use based on the PLAND scale is positive for all land-use, and as a result of increases in the percentage of impervious surfaces of the city, LST has increased.

LPI has negative implications for vegetation in all land-use except industrial, resulting in less percentage and less land-coverage. Removing and reducing the size of the green patches will increase the number of patches in the impacted surfaces of the city. By reducing the size of the green cover, conditions for creating thermal islands are met. On the other hand, with the increase of patches of impervious surfaces of the urban regions, the intensity of thermal islands will rise. ED actually examines the complexity and simplicity of urban spots. Whatever the complexity of the impervious lands, its relationship with the surface temperature will be positive and will be negative for vegetation (Table 3).

The results of this measure have shown that, with increasing complexity of shape and density of edges in impervious surfaces, LST has also increased. The results showed that the highest edge density for impervious surfaces was for the Ministerial-Commercial land-use, which had the highest positive correlation with LST and for vegetation cover. The highest edges were observed in the Educational-Health land-use and had the most negative correlation with LST.

Increasing PD in impervious surfaces means less variation of other land-covers. The relationship between compression and surface temperature in impervious surfaces is positive, in other words, increases in number of impervious surfaces as well as the density of their patches will result in further increment in surface temperature. However, this relationship has been negative in administrative-commercial lands due to low number of impervious lands. The relationship between PD for vegetated land-cover and surface temperature was negative in all land-uses (Table 3).

Increases in MPS value are indicative of high integral patches, whereas reductions in MPS, show the need for splitting the patches, causing heterogeneity in the spikes, thereby increasing the average temperature variation in land-use. This is the best interpreter for patch interconnection on the surface of the land. The negative relationship between green vegetation in different uses other than industrial indicates that the level of surface temperature decreases as the amount of MPS increases. The main reason behind the positive correlation between vegetation in industrial use and the surface temperature of the earth is due to increased fragmentation of vegetation and the very low area of vegetation in this land-use. The relationship between impervious surfaces based on MPS measurements exists in all land-use with

surface temperature, which results in the integrity of impervious surfaces in different land-use.

4. Discussion

4.1. Relationship between LST and land-cover

The map of impervious surfaces and vegetation is shown in Fig. 2. As can be observed from this figure, impervious surfaces and vegetation are the dominant land-covers in Urmia. Temperatures for impervious surfaces vary as shown in Fig. 3 from 29°C to 39.38°C, whereas temperatures for vegetation covers range between 20.60°C and 29°C. The reason for low temperatures in vegetation covers is due to the high energy demand of plants for solar energy as a means for their transpiration processes, which reduces the temperature as well as the amount of water present in the plants and the higher thermal capacity of the water compared to the other levels, and ultimately the effect of the shadow of buildings on vegetation, which reduces the average temperature in this land-cover (Li *et al.*, 2011). The average temperature of impervious surfaces is high, due to lower thermal capacity of impervious surfaces compared to other land-cover, such as vegetation, as well as industrial use and fossil fuels, and ultimately human activities in these types of land-cover.

The results of Table 3 and the relationship between vegetation and impervious surfaces with LST are indicative of the negative correlation between vegetation and LST (Weng *et al.*, 2004; Yuan and Bauer, 2007) as well as the positive correlation between impervious surfaces and surface temperatures (Yuan and Bauer, 2007; Li *et al.*, 2011). However, the correlation coefficient of the land-cover in various land-uses was different from LST.

The analysis of the land-cover area and the shape of the regions alongside the dispersion of patches, as shown in Figure 2, indicates impervious lands as highest in terms of surface area. These levels are patches of great connectivity. Therefore, according to the positive relationship between impervious surfaces and surface temperature, shape, area and distribution of impervious surfaces in Urmia, impervious surfaces can be said to be the main factor in increasing the city's average temperature. Vegetation cover, due to its relationship with impervious surfaces is an effective factor in reducing the city's average temperature, however it should be noted that the surface area of this land-cover is significantly important in reducing the urban thermal island (Chang *et al.*, 2007; Lee

et al., 2009). Vegetation surface area is very low compared to impervious surfaces, and the size of its parts are small and the connection between the parts is very sparse. Therefore, its role in reducing the average temperature is weak. Finally, it can be said that the role of impervious surfaces in increasing the mean surface temperature is much higher than the effect of vegetation in reducing the city's average temperature.

4.2. Land-use analysis and its relationship with LST

The range of LST alterations is extremely variable based on land-use (Fig. 3). Thus, land-cover is not an accurate measure of changes in LST, highlighting the need to consider land-use as a means for showing changes in LST. As mentioned in previous studies, LULC are effective on thermal islands, however, LULC configurations should also be considered (Connors et al., 2013). The configuration features are in fact related to the type of parts, spots and the type of LULC (Connors et al., 2013; Turner et al., 2001). A review of the configuration features is possible using Landscape Metrics (Gustafson, 1998), which was considered in this study.

Area analysis and land-use have been investigated with respect to increasing and decreasing effects on the city's average temperature (Table 2). As shown in table 2, LFF residential and industrial users have the lowest temperature and the highest average temperature, respectively, underlining the importance of land-use in changes in LST. Administrative-commercial and Educational-health care, with a high average temperature and a higher surface area, play an important role in increasing the average LST. The use of FFM residential, which largely reflects the role of urban geometry, has a higher average temperature than that of LFF residential, which in addition to the role of higher altitude, results in higher population density and human activity.

Impervious land-cover in LFF and FFM, based on all Landscape Metrics, had a positive relationship with LST, in contrast to vegetation, which had a negative relation with LST. The mean negative correlation of vegetation in FFM was greater compared to LFF, which is the result of the shadow effect of higher buildings in the vegetated land-cover (Li et al., 2011). Also, the mean positive correlation between impervious surfaces with LST in FFM was greater than LFF, chiefly due to higher population densities and the effect of height and urban geometry on the

increase in mean LST (Nakata-Osaki et al., 2018).

According to all Landscape Metrics for the Industrial use, there is a positive relationship between vegetation and surface temperature. In the industrial use, vegetation has little impact on impervious lands, as well as increased human activity and fossil fuels due to the increase in average temperature. Therefore, industrial use at the city level is one of the important factors in creating thermal island. The results of LULC analysis have shown that in addition to impervious lands, which have led to an increase in the average temperature of Urmia, the existence of industrial lands, high population density in administrative-commercial applications, and the effect of height and geometry in FFM use have also been major contributors to the creation of thermal island.

Table 3 shows how the average temperature varies based on each kind of land-use, which is due to the different effects of each type of land-cover; therefore, the identification of the effects of land-use and the different covers on changes in LST with respect to landscape metrics, as in previous studies (Li et al., 2013; Connors et al., 2013) is needed for urban management and planning. The results of table 3 show little correlation between land-cover type in different land-uses and LST, which is consistent with the results of other studies (Zhou et al., 2011; Li et al., 2011; Li et al., 2013). The highest average temperature is related to industrial use. Industrial uses, consume a lot of energy and therefore generate a lot of heat (Sailor, 2011) resulting in higher temperatures compared to other uses. Industrial uses have a lower percentage of vegetation than commercial-administrative uses; hence, the average temperature, caused by the inverse effect of vegetation on LST is higher (Hu and Jia, 2010).

Energy consumption and heat emission as a result of human activities are also effective on LST and in some land-uses have caused differences in thermal mean. In previous studies it was mentioned that human activities, human body metabolism and traffic caused a considerable increase in the temperature of urban environments (Sailor, 2011; Smith et al., 2009). The effects of human activities were significantly influential on increased mean temperature in FFM residential lands compared to LFF residential lands.

In comparing LFF residential lands with FFM residential lands, vertical development of buildings, increasing number of floors and as a result, and increased density of human activity have resulted in rising LSTs (Li et al., 2014) of

FFM residential areas compared to LFF residential lands. Therefore, human activities in different land-uses are considered as one of the effective factors in intensifying the thermal island effect.

Finally, the results indicate that there are similar temperatures in land-uses with similar land-cover. This suggests that, in addition to land-cover, other conditions also control the surface temperature, which are more related to the types of land-uses and population density and relevant activities. The results also showed that impervious surfaces had a direct relationship with surface temperature in all land-uses, while vegetation was only directly related to surface temperature for industrial use and indirectly related to LST for other land-uses.

4.3. Urban planning and land-use/land-cover management

Urban heat island is one of the most alarming environmental hazards in urban areas, with direct and indirect impacts on urban climate. Unfortunately, in most countries, the phenomenon of urban heat is not considered as a serious threat.

The relationship between LST and LULC with respect to Landscape Metrics is significantly important in urban planning and reduction of thermal islands (Li *et al.*, 2011). Urbanization is complicated by land-use (Weng *et al.*, 2007; Yu and Ng, 2007), which can have varying effects on LST changes. The results of this study showed that the island's thermal intensity is largely dependent on the area, the shape and the interconnectedness of impervious surfaces and vegetation cover. In Urmia, the largest part of the impervious surfaces includes the large and interconnected parts. The effects of these parts on increasing LST are much greater than the role of vegetation in reducing LST. The results from Landscape Metrics also show that impervious surfaces have a positive relationship with LST for almost all land-use, and the greater the density of parts. The percentage of impervious surfaces and the increased complexity of the parts, the higher the growth of the island. However, vegetation showed no negative relationship with LST in all land-uses, resulting in less area, smaller parts, and lack of interconnection of parts for this land-use, which as a result has caused further increases in the thermal island of Urmia.

According to the results, it is therefore necessary to present certain strategies to reduce the thermal island of Urmia. Replacing vegetation with impervious surfaces through the

use of green roofs and green walls, which in addition to reducing the thermal islands in the city (Dwivedi and Mohan, 2018), reduce greenhouse gases, increases oxygen production and strokes the air as well as decreases poverty (Rowe, 2011; Li and Babcock, 2014). Increasing vegetation cover and the construction of parks alongside land-uses that have a high LST can also help reduce the thermal island (Šuklje *et al.*, 2016). Considering the role of the height of buildings and urban geometry in increasing the intensity of the thermal island (Nakata-Osaki *et al.*, 2018; Rezaei Rad *et al.*, 2017), it is possible to construct buildings of lower heights in the future. Finally, taking into account that impervious surfaces have a high surface area, the use of high reflection materials and white roofs will play an important role in reducing the average temperature of Urmia (Akbari *et al.*, 2007; Sharma *et al.*, 2017).

5. Conclusion

This study thoroughly analyzed the effects of land-cover and land-use on LST for the case of Urmia City. Impervious surfaces, as the dominant cover (79.75%) alongside vegetation, with a negligible percentage (6.02%) were the two main coatings of the city of Urmia which have had important impacts on the thermal island of the city (Given that we know Vegetation mitigates LST, while impervious increases it). On the other hand, LFF residential, FFM residential, administrative-commercial, industrial, and educational-health-care applications have had a different impact on LST changes with each of them including two major land-covers (impervious and vegetated land-cover). The study shows that LULC have different impacts on LST. It was also shown that factors important affecting urban LST are not limited to only land-cover patterns, but also include other anthropogenic forces. Therefore, to identify these effects and provide solutions, it was necessary to carefully examine the effects of LULC using Landscape Metrics and fine resolution images. The results showed that, given the area, shape and coherence of impervious surfaces and vegetation in the study area, the impact of impervious surfaces in increasing LST was significantly more than the effect of vegetation on LST reduction. These outcomes were further verified by the results obtained for different land-uses.

The average temperature variation of different uses has shown that industrial and administrative-commercial lands have the highest average temperature due to industrial

activities and the increase of fossil fuels in industrial applications as well as increases in population density and human activities in the administrative- commercial. The lowest average temperatures were observed in the LFF residential and FFM residential use. The higher average temperature of FFM residential compared to LFF residential was due to larger population density and the role of elevation and building morphology in increasing the average temperature of FFM residential lands. Therefore, high density high-rise residential areas should be avoided in urban planning. Furthermore, increasing vegetation by locating and constructing parks, covering concrete structures with green facades (Šuklje *et al.*, 2016) and the use of reflecting surfaces in these structures can play a major role in absorbing and reflecting solar radiation and thus reducing island heat in the city.

Acknowledgments

The authors would like to thank Iran's National Elites Foundation for supporting this study. Free satellite data were kindly provided by the US Geological Survey (USGS). Finally, we thank the reviewers for their constructive comments and suggestions on the earlier versions of the manuscript.

References

- Akbari, H., S. Menon, A. Rosenfeld, 2007. Global Cooling: Effect Of Urban Albedo On Global Temperature. Ernest Orlando Lawrence Berkeley National Laboratory, Berkeley, Ca (Us).
- Alavipanah, S. K., M. K. Mogaddam, M. K. Firozjaei, 2017. Monitoring spatiotemporal changes of heat island in babol city due to land use changes. *International archives of the photogrammetry, remote sensing & spatial information sciences*, vol. 42, <https://doi.org/10.5194/isprs-archives-xlii-4-w4-17-2017>
- Amiri, R., Q., Weng, A. Alimohammadi, S. K. Alavipanah, 2009. Spatial–Temporal Dynamics Of Land Surface Temperature In Relation To Fractional Vegetation Cover And Land-Use/Cover In The Tabriz Urban Area, Iran. *Remote Sensing Of Environment*, 113, 2606-2617.
- Arnold Jr, C. L. C. J. Gibbons, 1996. Impervious Surface Coverage: The Emergence Of A Key Environmental Indicator. *Journal Of The American Planning Association*, 62, 243-258.
- Artis, D. A., W. H. Carnahan, 1982. Survey Of Emissivity Variability In Thermography Of Urban Areas. *Remote Sensing Of Environment*, 12, 313-329.
- Bottyán, Z., J. Unger, 2003. A Multiple Linear Statistical Model For Estimating The Mean Maximum Urban Heat Island. *Theoretical And Applied Climatology*, 75, 233-243.
- Bruns, J., V. Simko, 2017. Stable Hotspot Analysis For Intra-Urban Heat Islands. *Gi_Forum, Salzburg, Austria. Google Scholar*.
- Cenedese, A., P. Monti, 2003. Interaction Between An Inland Urban Heat Island And A Sea-Breeze Flow: A Laboratory Study. *Journal Of Applied Meteorology*, 42, 1569-1583.
- Chang, C.-R., M.-H. Li, S.-D. Chang, 2007. A Preliminary Study On The Local Cool-Island Intensity Of Taipei City Parks. *Landscape And Urban Planning*, 80, 386-395.
- Connors, J. P., C. S. Galletti, W. T. L. Chow, 2013. Landscape Configuration And Urban Heat Island Effects: Assessing The Relationship Between Landscape Characteristics And Land Surface Temperature In Phoenix, Arizona. *Landscape Ecology*, 28, 271-283.
- De Faria Peres, L., A. J. De Lucena, O. C. Rotunno Filho, J. R. De Almeida Franca, 2018. The Urban Heat Island In Rio De Janeiro, Brazil, In The Last 30 Years Using Remote Sensing Data. *International Journal Of Applied Earth Observation And Geoinformation*, 64, 104-116.
- Du, Z., W. Li, D. Zhou, L. Tian, F. Ling, H. Wang, Y. Gui, B. Sun, 2014. Analysis Of Landsat-8 Oli Imagery For Land Surface Water Mapping. *Remote Sensing Letters*, 5, 672-681.
- Dwivedi, A., Mohan, K. Buddhiraju, 2018. Impact Of Green Roof On Micro Climate To Reduce Urban Heat Island. *Remote Sensing Applications: Society And Environment*, 10, 56-69.
- Estoque, R. C., Y. Murayama, 2013. Landscape Pattern And Ecosystem Service Value Changes: Implications For Environmental Sustainability Planning For The Rapidly Urbanizing Summer Capital Of The Philippines. *Landscape And Urban Planning*, 116, 60-72.
- Estoque, R. C., Y. Murayama, 2015. Classification And Change Detection Of Built-Up Lands From Landsat-7 Etm+ And Landsat-8 Oli/Tirs Imageries: A Comparative Assessment Of Various Spectral Indices. *Ecological Indicators*, 56, 205-217.
- Ezimand, K., A. A. Kakroodi, M. Kiavarz, 2018. The Development Of Spectral Indices For Detecting Built-Up Land Areas And Their Relationship With Land-Surface Temperature. *International Journal Of Remote Sensing*, 1-22.
- Farina, A., 2012. Exploring The Relationship Between Land Surface Temperature And Vegetation Abundance For Urban Heat Island Mitigation In Seville, Spain. *Luma-Gis Thesis*.
- Goward, S. N., Y. Xue, K. P. Czajkowski, 2002. Evaluating Land Surface Moisture Conditions From The Remotely Sensed Temperature/Vegetation Index Measurements: An Exploration With The Simplified Simple Biosphere Model. *Remote Sensing Of Environment*, 79, 225-242.
- Gustafson, E. J., 1998. Quantifying Landscape Spatial Pattern: What Is The State Of The Art? *Ecosystems*, 1, 143-156.
- Hakimzadeh Ardakania, M.A., A.R. Vahdati, 2018. Monitoring of organic matter and soil salinity by using IRS - LissIII satellite data in the Harat plain, of Yazd province. *Desert*, 23, 1-8.
- Han-Qiu, X., C. Ben-Qing, 2004. Remote Sensing Of The Urban Heat Island And Its Changes In Xiamen City Of Se China. *Journal Of Environmental Sciences*, 16, 276-281.

- Herath, H. M. P. I. K., R. U. Halwatura, G. Y. Jayasinghe, 2018. Modeling A Tropical Urban Context With Green Walls And Green Roofs As An Urban Heat Island Adaptation Strategy. *Procedia Engineering*, 212, 691-698.
- Hu, Y., G. Jia, 2010. Influence Of Land-Use Change On Urban Heat Island Derived From Multi-Sensor Data. *International Journal Of Climatology*, 30, 1382-1395.
- Jiang, X.-D., B.-C. Xia, L. Guo, 2006. Research On Urban Heat Island And Its Environmental Effects Of Rapidly Urbanized Regions. *Ecologic Science*, 2, 021.
- Jimenez-Muñoz, J. C., J. A. Sobrino, 2003. A Generalized Single-Channel Method For Retrieving Land Surface Temperature From Remote Sensing Data. *Journal Of Geophysical Research: Atmospheres*, 108.
- Kassa, A., 1999. Drought Risk Monitoring For Sudan Using Ndvi 1982-1993.
- Keshtkar, H.R. 2008. Investigation Of The Capability Of IRS Satellite Data For Land Cover Mapping. *Ms.C Thesis. University Of Tehran*.
- Keshtkar, H.R., H. Azarnivand, H. Arzani, S. Alavipanah, 2013. Land-Cover Classification Using IRS-1D Data And A Decision Tree Classifier. *Desert*, 17(2), 137-146.
- Keshtkar, H., W. Voigt, E. Alizadeh, 2017. Land-Cover Classification And Analysis Of Change Using Machine-Learning Classifiers And Multi-Temporal Remote Sensing Imagery. *Arab. J. Geosci.* 10(6), 154.
- Kong, F., N. Nakagoshi, 2006. Spatial-Temporal Gradient Analysis Of Urban Green Spaces In Jinan, China. *Landscape And Urban Planning*, 78, 147-164.
- Kourosh Niya, A., J. Huang, H. Karimi, H. Keshtkar, B. Naimi, 2019. Use of Intensity Analysis to Characterize Land Use/Cover Change in the Biggest Island of Persian Gulf, Qeshm Island, Iran. *Sustainability*, 11, 4396.
- Lee, S.-H., K.-S. Lee, W.-C. Jin, H.-K. Song, 2009. Effect Of An Urban Park On Air Temperature Differences In A Central Business District Area. *Landscape And Ecological Engineering*, 5, 183-191.
- Li, J., C. Song, L. Cao, F. Zhu, X. Meng, J. Wu, 2011. Impacts Of Landscape Structure On Surface Urban Heat Islands: A Case Study Of Shanghai, China. *Remote Sensing Of Environment*, 115, 3249-3263.
- Li, W., Y. Bai, Q. Chen, K. He, X. Ji, C. Han, 2014. Discrepant Impacts Of Land-Use And Land-Cover On Urban Heat Islands: A Case Study Of Shanghai, China. *Ecological Indicators*, 47, 171-178.
- Li, X., W. Li, A. Middel, S. L. Harlan, A. J. Brazel, B. L. Turner, 2016. Remote Sensing Of The Surface Urban Heat Island And Land Architecture In Phoenix, Arizona: Combined Effects Of Land Composition And Configuration And Cadastral-Demographic-Economic Factors. *Remote Sensing Of Environment*, 174, 233-243.
- Li, X., W. Zhou, Z. Ouyang, 2013. Relationship Between Land Surface Temperature And Spatial Pattern Of Greenspace: What Are The Effects Of Spatial Resolution? *Landscape And Urban Planning*, 114, 1-8.
- Li, Y., R. W. Babcock, 2014. Green Roofs Against Pollution And Climate Change. A Review. *Agronomy For Sustainable Development*, 34, 695-705.
- Liu, L., Y. Zhang, 2011. Urban Heat Island Analysis Using The Landsat Tm Data And Aster Data: A Case Study In Hong Kong. *Remote Sensing*, 3, 1535-1552.
- Luck, M., J. Wu, 2002. A Gradient Analysis Of Urban Landscape Pattern: A Case Study From The Phoenix Metropolitan Region, Arizona, Usa. *Landscape Ecology*, 17, 327-339.
- Maimaitiyiming, M., A. Ghulam, T. Tiyp, F. Pla, P. Latorre-Carmona, Ü. Halik, M. Sawut, M. Caetano, 2014. Effects Of Green Space Spatial Pattern On Land Surface Temperature: Implications For Sustainable Urban Planning And Climate Change Adaptation. *Isprs Journal Of Photogrammetry And Remote Sensing*, 89, 59-66.
- Mcgarigal, K., S. A. Cushman, M. C. Neel, E. Ene, 2002. Fragstats: Spatial Pattern Analysis Program For Categorical Maps.
- Nakata-Osaki, C. M., L. C. L. Souza, D. S. Rodrigues, 2018. This-Tool For Heat Island Simulation: A Gis Extension Model To Calculate Urban Heat Island Intensity Based On Urban Geometry. *Computers, Environment And Urban Systems*, 67, 157-168.
- Nonomura, A., M. Kitahara, T. Masuda, 2009. Impact Of Land-Use And Land-Cover Changes On The Ambient Temperature In A Middle Scale City, Takamatsu, In Southwest Japan. *Journal Of Environmental Management*, 90, 3297-3304.
- Oke, T. R., R. Spronken-Smith, E. Jáuregui, C. S. Grimmond, 1999. The Energy Balance Of Central Mexico City During The Dry Season. *Atmospheric Environment*, 33, 3919-3930.
- Owen, T., T. Carlson, R. Gillies, 1998. An Assessment Of Satellite Remotely-Sensed Land-Cover Parameters In Quantitatively Describing The Climatic Effect Of Urbanization. *International Journal Of Remote Sensing*, 19, 1663-1681.
- Quan, J., Y. Chen, W. Zhan, J. Wang, J. Voogt, M. Wang, 2014. Multi-Temporal Trajectory Of The Urban Heat Island Centroid In Beijing, China Based On A Gaussian Volume Model. *Remote Sensing Of Environment*, 149, 33-46.
- Rezaei Rad, H., M. Rafieian, H. Sozer, 2017. Evaluating The Effects Of Increasing Of Building Height On Land Surface Temperature. *International Journal Of Urban Management And Energy Sustainability*, 1, 11-16.
- Rimal, B., L. Zhang, H., Keshtkar, B. N. Haack, S. Rijal, P. Zhang, 2018. Land-Use/Land-Cover Dynamics And Modeling Of Urban Land Expansion By The Integration Of Cellular Automata And Markov Chain. *Isprs International Journal Of Geo-Information*, 7, 154.
- Rimal, B., H. Keshtkar, R. Sharma, N. Stork, S. Rijal, R. Kunwar, 2019a. Simulating urban expansion in a rapidly changing landscape in eastern Tarai, Nepal. *Environ Monit Assess*, 191: 255.
- Rimal, B., R. Sharma, R. Kunwar, H. Keshtkar, N. Stork, S. Rijal, S.A. Rahman, H. Baral, 2019b. Effects of land use and land cover change on ecosystem services in the Koshi River Basin, Eastern Nepal. *Ecosystem Services*, 38: 100963.
- Rouse Jr, J. W., R. Haas, J. Schell, D. Deering, 1974. Monitoring Vegetation Systems In The Great Plains With Ert's.
- Rowe, D. B., 2011. Green Roofs As A Means Of Pollution Abatement. *Environmental Pollution*, 159, 2100-2110.
- Sailor, D. J., 2011. A Review Of Methods For Estimating Anthropogenic Heat And Moisture Emissions In The Urban Environment. *International Journal Of Climatology*, 31, 189-199.
- Sharma, S., A. S. Ajai Kiran Kumar, 2017. Effect Of Urban Surface Albedo Enhancement In India On

- Regional Climate Cooling. *Remote Sensing Applications: Society And Environment*, 8, 193-198.
- Shen, H., L. Huang, L. Zhang, P. Wu, C. Zeng, 2016. Long-Term And Fine-Scale Satellite Monitoring Of The Urban Heat Island Effect By The Fusion Of Multi-Temporal And Multi-Sensor Remote Sensed Data: A 26-Year Case Study Of The City Of Wuhan In China. *Remote Sensing Of Environment*, 172, 109-125.
- Smith, C., S. Lindley, G. Levermore, 2009. Estimating Spatial And Temporal Patterns Of Urban Anthropogenic Heat Fluxes For Uk Cities: The Case Of Manchester. *Theoretical And Applied Climatology*, 98, 19-35.
- Streutker, D. R., 2002. A Remote Sensing Study Of The Urban Heat Island Of Houston, Texas. *International Journal Of Remote Sensing*, 23, 2595-2608.
- Streutker, D. R., 2003. Satellite-Measured Growth Of The Urban Heat Island Of Houston, Texas. *Remote Sensing Of Environment*, 85, 282-289.
- Šuklje, T., S. Medved, C. Arkar, 2016. On Detailed Thermal Response Modeling Of Vertical Greenery Systems As Cooling Measure For Buildings And Cities In Summer Conditions. *Energy*, 115, 1055-1068.
- Taha, H., 1997. Urban Climates And Heat Islands: Albedo, Evapotranspiration, And Anthropogenic Heat. *Energy And Buildings*, 25, 99-103.
- Turner, M. G., R. H. Gardner, R. V. O'neill, 2001. Landscape Ecology In Theory And Practice: Patterns And Process. *Eua: Springer*.
- Van De Griend, A., M. Owe, 1993. On The Relationship Between Thermal Emissivity And The Normalized Difference Vegetation Index For Natural Surfaces. *International Journal Of Remote Sensing*, 14, 1119-1131.
- Weng, Q., 2001. A Remote Sensing? Gis Evaluation Of Urban Expansion And Its Impact On Surface Temperature In The Zhujiang Delta, China. *International Journal Of Remote Sensing*, 22, 1999-2014.
- Weng, Q., 2003. Fractal Analysis Of Satellite-Detected Urban Heat Island Effect. *Photogrammetric Engineering Remote Sensing*, 69, 555-566.
- Weng, Q., 2009. Thermal Infrared Remote Sensing For Urban Climate And Environmental Studies: Methods, Applications, And Trends. *Isprs Journal Of Photogrammetry And Remote Sensing*, 64, 335-344.
- Weng, Q., H. Liu, D. Lu, 2007. Assessing The Effects Of Land-Use And Land-Cover Patterns On Thermal Conditions Using Landscape Metrics In City Of Indianapolis, United States. *Urban Ecosystems*, 10, 203-219.
- Weng, Q., D. Lu, J. Schubring, 2004. Estimation Of Land Surface Temperature-Vegetation Abundance Relationship For Urban Heat Island Studies. *Remote Sensing Of Environment*, 89, 467-483.
- Wu, C., 2004. Normalized Spectral Mixture Analysis For Monitoring Urban Composition Using Etm+ Imagery. *Remote Sensing Of Environment*, 93, 480-492.
- Wu, J., G. D. Jenerette, A. Buyantuyev, C. L. Redman, 2011. Quantifying Spatiotemporal Patterns Of Urbanization: The Case Of The Two Fastest Growing Metropolitan Regions In The United States. *Ecological Complexity*, 8, 1-8.
- Xiao, J., A. Moody, 2005. A Comparison Of Methods For Estimating Fractional Green Vegetation Cover Within A Desert-To-Upland Transition Zone In Central New Mexico, Usa. *Remote Sensing Of Environment*, 98, 237-250.
- Xunqiang, M., C. Chen, Z. Fuqun, L. Hongyuan, 2011. Study On Temporal And Spatial Variation Of The Urban Heat Island Based On Landsat Tm/Etm+ In Central City And Binhai New Area Of Tianjin. Multimedia Technology (Icmt), International Conference On, 2011. Ieee, 4616-4622.
- Yu, X. J., C. N. Ng, 2007. Spatial And Temporal Dynamics Of Urban Sprawl Along Two Urban-Rural Transects: A Case Study Of Guangzhou, China. *Landscape And Urban Planning*, 79, 96-109.
- Yuan, F., M. E. Bauer, 2007. Comparison Of Impervious Surface Area And Normalized Difference Vegetation Index As Indicators Of Surface Urban Heat Island Effects In Landsat Imagery. *Remote Sensing Of Environment*, 106, 375-386.
- Yousefi, S., S. Mirzaee, M. Tazeh, H. Pourghasemi, H. Karimi, 2015. Comparison of different algorithms for land use mapping in dry climate using satellite images: a case study of the Central regions of Iran. *Desert*, 20(1), 1-10.
- Zhou, W., G. Huang, M. L. Cadenasso, 2011. Does Spatial Configuration Matter? Understanding The Effects Of Land-Cover Pattern On Land Surface Temperature In Urban Landscapes. *Landscape And Urban Planning*, 102, 54-63.